CHEMISTRY OF MATERIALS
Article

Chem. Mater. **2010,** *22,* 5887–5894 5887
DOI:10.1021/cm101970b

Surfactant-Induced Electrodeposition of Layered Manganese Oxide with Large Interlayer Space for Catalytic Oxidation of Phenol

Masaharu Nakayama,* Mitsuhiro Shamoto, and Akio Kamimura

Department of Applied Chemistry, Yamaguchi University, 2-16-1 Tokiwadai, Ube 755-8611, Japan

Received July 15, 2010. Revised Manuscript Received September 23, 2010

Electrolysis of aqueous Mn^{2+} ions at an anodic potential of +1.0 V (vs Ag/AgCl) in the presence of cationic surfactants led to the formation of multilayered manganese oxides intercalated with the surfactant molecules. Their interlayer spacings are much larger than that (~0.7 nm) of conventional birnessite; i.e., 3.1 nm with cetyltrimethyl ammonium (C16) and 2.4 nm with dodecyltrimethyl ammonium (C12). According to XPS analysis, the molar ratio of C16 to MnO_2 was estimated to be 0.74, in which the C16 fraction of 0.42 is associated with Cl^- anions and the other (0.32) interacts with negative charges on the Mn oxide layer. C16 surfactants accommodated between the Mn oxide layers were not ion-exchanged with Na^+ ions in solution but extracted with ethanol. Anodic oxidation of the C16-intercalated Mn oxide (C16/MnO_2) film took place in an aqueous Na_2SO_4 solution, accompanied with insertion of SO_4^{2-} anions for charge compensation, and not deintercalation of the surfactants. As a result, the layered structure with large interlayer space was maintained at anodic potentials. The C16/MnO_2 film effectively oxidized hydroquinone (HQ) to benzoquinone (BQ), in which the high-valent Mn sites (Mn^{4+}) in the oxide were reduced to Mn^{3+}. At open circuit potential, the low-valent Mn species were accumulated, leading to a collapse of the C16-intercalated structure within 250 min; however, applying an anodic potential allowed the structure to remain unchanged, in conjunction with the acceleration of HQ oxidation. This can be attributed to the reoxidation of the Mn^{3+} ions resulting from HQ oxidation, keeping the charge in the oxide so that the surfactants are not necessary to be deintercalated. Namely, the MnO_2 layer can act as an electron-transfer mediator for the oxidation of HQ occurring in the large interlayer space. The observed catalytic current was 684 times larger than the current observed on the unmodified electrode.

Introduction

Manganese oxide materials, especially manganese dioxide (MnO_2), are very attractive because of their distinctive structures and physicochemical properties as well as environmental compatibility and cost effectiveness. A great deal of attention has been devoted to the application of Mn oxides in a variety of fields, such as adsorbents, catalysis, batteries, and recently supercapacitors. Among various Mn dioxide polymorphs such as α-, *β*-, *γ*-, and *δ*-MnO_2, birnessite (*δ*-MnO_2) has attracted particular attention owing to its unique catalytic properties. Birnessite is a naturally occurring mineral having a layered structure composed of the edge-shared MnO_6 octahedra containing predominantly Mn^{4+} cations as the center ions. Some of the Mn^{4+} ions are replaced with Mn^{3+} ions, giving a net negative charge to be compensated by the intercalation of guest cations, usually hydrated alkaline metals. The interlayer distance is typically about 0.7 nm. Catalytic activity of birnessite, which mainly arises from Mn^{4+} ions, has been found in the oxidation of alcohols,[1] iodine,[2] phenolic compounds,[3−5] etc. In such cases, leaching of the reduced Mn species must be avoided in order to maintain the catalytic ability. Phenolic compounds such as hydroquinone, catechol, and resorcinol are discharged to the environment from a variety of industries because they are used in the production of rubber, dyes, pesticides, colors, plastics, and cosmetics. Thus, electrochemical oxidation of phenolic compounds is an important process in the analytical detection of phenols and in the oxidative decomposition of phenol impurities in aqueous systems.[6−8]

A wide variety of chemical methods have so far been developed for the synthesis of birnessite[9−11] until we first reported a facile electrochemical route[12,13] to build birnessite

*Author to whom correspondence should be addressed. Tel: +81-836-9223. Fax: +81-836-85-9201. E-mail: nkymm@yamaguchi-u.ac.jp.

(1) Son, Y.-C.; Makwana, V. D.; Howell, A. R.; Suib, S. L. *Angew. Chem., Int. Ed.* **2001**, *40*, 4280.
(2) Allard, S.; Gunten, U.; Sahli, E.; Nicolau, R.; Gallard, H. *Water Res.* **2009**, *43*, 3417.
(3) Hardie, A. G.; Dynes, J. J.; Kozak, L. M.; Huang, P. M. *J. Mol. Catal. A: Chem.* **2009**, *308*, 114.
(4) Chan Chien, S. W.; Chen, H. L.; Wang, M. C.; Seshaiah *Chemosphere* **2009**, *74*, 1125.
(5) Rao, M. A.; Iamarino, G.; Scelza, R.; Russo, F.; Gianfreda, L. *Sci. Total Environ.* **2008**, *407*, 438.
(6) Prado, C.; Murcott, G. G.; Marken, F.; Foord, J. S.; Compton, R. G. *Electroanalysis* **2002**, *14*, 975.
(7) Canizares, P.; Martinez, F.; Diaz, M.; Garcia-Gomez, J.; Rodrigo, M. A. *J. Electrochem. Soc.* **2002**, *149*, D118.
(8) Wang, Y.; Gu, B.; Xu, W. *J. Hazard. Mater.* **2009**, *162*, 1159.
(9) Ching, S.; Petrovay, D. J.; Jorgensen, M. L.; Suib, S. L. *Inorg. Chem.* **1997**, *36*, 883.
(10) Shen, Y. F.; Suib, S. L.; O'Young, C. L. *J. Am. Chem. Soc.* **1994**, *116*, 11020.
(11) Luo, J.; Suib, S. L. *Chem. Commun.* **1997**, 1031.

Published on Web 10/12/2010

as a thin film. The process involves a potentiostatic oxidation of aqueous Mn^{2+} ions in the presence of different guest molecules. This methodology is totally different from the surfactant templating route developed by other research groups to create mesostructured transition metal oxides, including NiO,[14,15] ZnO,[16] Cu_2O,[17] and MnO_2,[18] where precursor metal ions adsorbed on the self-assembled nonionic or anionic surfactants are electrolyzed. Unlike the conventional chemical methods, electrochemical deposition can give rise to thin uniform films rather than powdery morphology, thus meeting the growing demands of more advanced thin films for electrochemical and sensor devices. Our electrochemical process for the Mn oxide formation can be represented by eq 1,[19] referring to the usual electrodeposition of MnO_2 ($Mn^{2+} + 2H_2O \rightarrow MnO_2 + 4H^+ + 2e^-$)

$$Mn^{2+} + 2H_2O + xA^+ \rightarrow A_xMn^{3+}{}_xMn^{4+}{}_{1-x}O_2 + 4H^+ + (2\text{-}x)e^- \quad (1)$$

where A^+ corresponds to cation. x represents the fraction of trivalent species in the oxide which is equivalent to the A^+/Mn ratio, while the fraction of tetravalent species is $1-x$.

The deposition mechanism consists of anodic formation of MnO_2 and the simultaneous assembly of electrolyte cations to negative charges on the deposited MnO_2. This approach is quite versatile because the inorganic host (MnO_2) can adjust itself to accommodate guest molecules during electrodeposition. In such a layered structure, all of the material can be regarded as "surfaces", and bicontinuous networks of solid and pore at the nanometer scale enable both electrons and cations to move fast and reversibly.[20] Such features have been reflected in the high performance of birnessite as a pseudocapacitor electrode.[21,22] Moreover, we reported an electron transfer into/from intercalated molecules, methylviologen dications, through the MnO_2 layer.[23] Thus, if we can insert the large organic molecules between the MnO_2 layers, there will be a "nano-sized" reaction field, especially for organic substances that are soluble in water. This situation can be regarded as a nanoreactor filled with organic solvent where electrons can be injected/ejected if the structure can be maintained during the reaction.

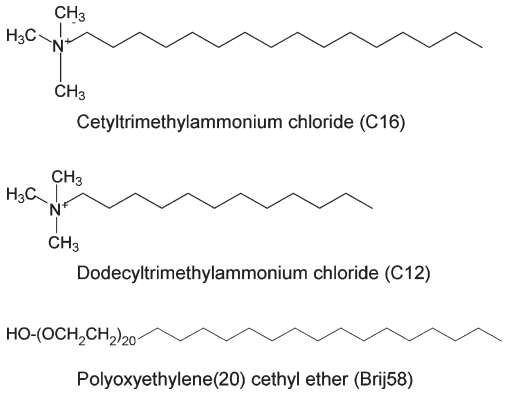

Figure 1. Structures of the surfactants used.

In the present study, we electrodeposited thin films of layered MnO_2 intercalated with cationic surfactants. Products were characterized in detail by spectroscopic and electrochemical techniques. Surfactant molecules in the interlayer do not act as individual ions but act collectively, resulting in a unique electrochemical behavior; i.e., they remained immobilized between the MnO_2 layers at anodic potentials. This property prompted us to examine the use of the resulting film electrode for oxidation of hydroquinone (HQ) with an electric field applied.

Experimental Section

Reagents and Chemicals. All chemicals were of reagent grade and used without any further purification. Surfactants, cetyltrimethylammonium chloride (C16, 95%), and dodecyltrimethyl ammonium chloride (C12, 97%) were obtained from Wako Pure Chemicals, and polyoxyethylene(20) cethyl ether (Brij58) were obtained from Aldrich. Their molecular structures are depicted in Figure 1. All solutions were prepared with doubly distilled water and were deoxygenated by bubbling purified nitrogen gas for at least 20 min prior to use.

Electrodeposition. Electrodeposition was carried out using a conventional three-electrode system in an undivided glass cell. A large surface area platinum sheet was used as the counter electrode, and a standard Ag/AgCl electrode (in saturated KCl) served as the reference electrode. An EG&G Princeton Applied Research Model 263A potentio/galvanostat was used to control the electrode potential. If not otherwise mentioned, an indium-doped tin oxide (ITO)-coated glass slide ($R = 10\ \Omega$ cm) with an active area of $2.0 \times 0.9\ cm^2$ was used as the working electrode to fabricate the films. For the reflection−absorption infrared and X-ray photoelectron spectroscopic measurements, a polycrystalline platinum sheet with a geometric area of $1.0 \times 1.0\ cm^2$ was used. Prior to electrodeposition, the electrode surface was ultrasonically cleaned in a mixed solution of ethanol and water and then rinsed thoroughly with distilled water. The deposition bath used consisted of 2 mM $MnSO_4$ aqueous solutions mixed with surfactants at various concentrations. A constant potential of +1.0 V was applied to the working electrode, while a fixed charge of 340 mC/cm^2 was delivered. This potential had been optimized to produce a film with the highest crystallinity. After electrodeposition, the resulting film coated on an electrode was rinsed thoroughly with water, dried under vacuum in a desiccator, and then subjected to spectroscopic and electrochemical measurements and phenol oxidation experiments.

(12) Nakayama, M.; Konishi, S.; Tanaka, A.; Ogura, K. *Chem. Lett.* **2004**, *33*, 670.
(13) Nakayama, M.; Tagashira, H.; Konishi, S.; Ogura, K. *Inorg. Chem.* **2004**, *43*, 8215.
(14) Nelson, P. A.; Elliott, J. M.; Attard, G. S.; Owen, J. R. *Chem. Mater.* **2002**, *14*, 524.
(15) Tan, Y.; Srinivasan, S.; Choi, K.-S. *J. Am. Chem. Soc.* **2005**, *127*, 3596.
(16) Choi, K.-S.; Lichtenegger, H. C.; Stucky, G. D.; McFarland, E. W. *J. Am. Chem. Soc.* **2002**, *124*, 12402.
(17) Luo, H. M.; Zhang, J. F.; Yan, Y. S. *Chem. Mater.* **2003**, *15*, 3769.
(18) Lee, C.-W.; Nam, K.-W.; Cho, B.-W.; Kim, K.-B. *Microporous Mesoporous Mater.* **2010**, *130*, 208.
(19) Nakayama, M.; Konishi, S.; Tagashira, H.; Ogura, K. *Langmuir* **2005**, *21*, 354.
(20) Long, J. W.; Qadir, L. R.; Stroud, R. M.; Rolison, D. R. *J. Phys. Chem. B* **2001**, *105*, 8712.
(21) Brousse, T.; Toupin, M.; Dugas, R.; Athouël, L. *J. Electrochem. Soc.* **2006**, *153*, A2171.
(22) Davaraj, S.; Munichandraiah, N. *J. Phys. Chem. C* **2008**, *112*, 4406.
(23) Nakayama, M.; Hoyashita, R.; Komatsu, H.; Muneyama, E.; Shoda, K.; Kunishige, A. *Langmuir* **2007**, *23*, 3462.

Structural Characterization. X-ray diffraction (XRD) patterns were recorded on a Rigaku Ultima IV diffractometer with Cu Kα radiation (λ = 0.154051 nm) as the X-ray source. The data were collected in a 2θ region from 1 to 60° at a scan rate of 1°/min. The beam voltage was 40 kV, while the beam current was 40 mA. A grazing incidence in-plane XRD study was performed with a four-axis goniometer (Rigaku ATX-G). IR spectroscopy was conducted on a Shimadzu FTIR 8400S. Reflection−absorption spectra of the deposited film on a Pt substrate were acquired at an angle of incidence of 80° using a reflectance accessory. Transmittance spectra of reagents were obtained using a pellet of the compound with KBr (Nacalai Tesque; IR grade). The resolution was 4 cm^{-1}, while 100 scans were collected. SEM images were obtained using a Hitachi S-4700Y microscope operating at 10 kV. Samples were observed directly without any coatings. Cross-sectional transmission electron microscope (TEM) observation was made using a JEOL JEM-CX 200 microscope at an accelerating voltage of 200 kV. X-ray photoelectron spectra (XPS) were collected using a JPS-9010MC spectrometer, with a Mg Kα (1253.6 eV) monochromatic source (15 kV, 20 mA). Wide- and narrow-range spectra were acquired with a pass energy of 20 eV and channel widths of 1.0 and 0.1 eV, respectively. The binding energy scale was calibrated with respect to the C 1s (284.5 eV) signal. Semiquantitative estimates of the relative atomic concentrations were obtained from the peak area ratios by considering the sensitivity factors provided by the instrument software.

Electrochemical Characterization. To elucidate electrochemical properties, the ITO electrode coated with the Mn oxide film was transferred to an aqueous solution of 0.5 M Na_2SO_4. Voltammetry was conducted in the same configuration as that used for the film preparation.

Phenol Oxidation. The film-coated ITO electrode was immersed in a quartz cuvette (10 mm path length) filled with 2.5 mL of an aqueous solution containing 0.3 mM HQ and 0.5 M Na_2SO_4. A Shimadzu UV2400PC spectrometer was used to monitor the optical absorption in solution. Polarization of the Mn oxide/ITO electrode was made in the same configuration where both reference and counter electrodes were placed outside the spectrometer beam.

Results and Discussion

Electrodeposition. Figure 2A displays XRD patterns of the films deposited on an ITO electrode in the presence of C16 (a), C12 (b), and Brij58 (c). The film deposited with nonionic Brij58 shows no peak at all except the substrate peaks (*), indicating X-ray amorphous. Clearly, nonionic surfactants are not involved in the nanostructuring process of Mn oxide. In the presence of C16, a set of evenly spaced seven peaks are observed, which is a diagnostic feature of layered structure. These peaks can be indexed to the 001 plane and its second- (002) to seventh- (007) order diffractions from multilayers of birnessite-type Mn oxide.[19] *d*-spacing of the 001 peak (d_{001}) corresponds to the interlayer spacing and was measured to be 3.1 nm according to Bragg's equation. C12 surfactant also provides similar diffractions up to third order with a smaller d_{001} spacing, 2.4 nm, where all the peaks are broader than the corresponding peaks in the film deposited with C16, indicating a less ordered structure. As we previously reported, similar electrodeposition with tetraalkylammonium cations ($(C_nH_{2n+1})_4N^+$: $n = 0 \sim 6$) yielded birnessite

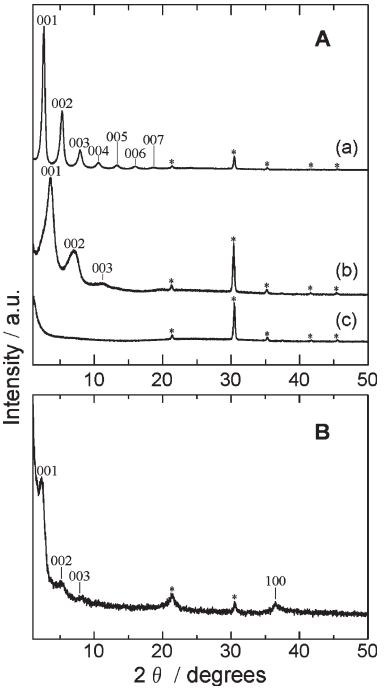

Figure 2. (A) XRD patterns of the films obtained from 2 mM $MnSO_4$ solutions containing 150 mM of (a) C16, (b) C12, and (c) Brij58 by applying a constant potential of +1.0 V. The electric charge passed during electrolysis was always 340 mC/cm^2. (B) In-plane XRD pattern of film a in part A.

films with diffraction peaks only up to third order.[12,13,19,24] Comparison of the product with C16 to those with other smaller cations strongly suggests that the multilayering process involves hydrophobic attraction between surfactants tails as well as the electrostatic interaction between their cationic heads and negative charges on the Mn oxide layers.

In-plane XRD measurement was conducted for the film with C16, as depicted in Figure 2B. A peak associated with an intrasheet reflection indexable to the 100 plane appears at 36.5°,[25,26] which is missing in curve a of Figure 2A. This indicates that each Mn oxide layer is crystallized neatly. Meanwhile, the 00*n* peaks are relatively weakened, implying that the Mn oxide layers lying parallel to the substrate surface are dominant over those directing perpendicular, which is consistent with TEM images shown later.

A film similarly prepared with C16 on a Pt substrate was subjected to IR analysis, and the obtained spectrum is shown in Figure 3a, along with that of pure C16 in a KBr pellet. Absorption peaks at 2926, 2852, 1469, 964, 914, and 721 cm^{-1} in the electrodeposited film can also be detected in the spectrum of the parent reagent. The OH bending and stretching vibrations in H_2O are observed at 1647 cm^{-1} and around 3400 cm^{-1}, respectively. A peak appearing at 634 cm^{-1} can be attributed to the stretching vibrations of Mn−O bond in Mn oxide.[27] Combined with

(24) Nakayama, M.; Fukuda, M.; Konishi, S.; Tonosaki, T. *J. Mater. Res.* **2006**, *21*, 3152.
(25) Julien, C.; Massot, M.; Baddour-Hadjean, R.; Franger, S.; Bach, S.; Pereira-Ramos *J. P. Solid State Ionics* **2003**, *159*, 345.
(26) Polzer, F.; Kunz, D. A.; Breu, J.; Ballauff, M. *Chem. Mater.* **2010**, *22*, 2916.

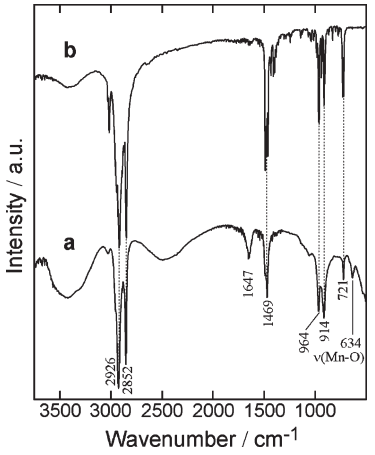

Figure 3. FTIR spectra of (a) the electrodeposited film from a 2 mM $MnSO_4$ solution with 150 mM C16 and (b) the C16 reagent in a KBr pellet.

the XRD pattern of film a in Figure 2A, C16 surfactant cations are accommodated between the Mn oxide layers. Hereafter, the birnessite-type Mn oxide film prepared with C16 surfactants is designated as C16/MnO_2. The film growth process can be recognized by the inorganic polymerization of MnO_2 and the simultaneous assembly of cationic surfactants to negative charges on the MnO_2 layers. Taking into account the crystallographic thickness of a MnO_2 layer (0.5 nm),[28] the interlayer spacings obtained with C16 (3.1 nm) and C12 (2.4 nm) correspond to gallery heights of 2.6 and 1.9 nm, respectively. Since the molecular sizes of C16 and C12 are 2.17 and 1.67 nm, respectively,[29] surfactants are accommodated in a form of single layer.

XPS wide-scan spectrum of the C16/MnO_2 film presented Mn 2p, O 1s, and Mn 3s signals arising from MnO_2 (Supporting Information, Figure S1). In the O 1s core-level spectrum, the contribution of O^{2-} (528.7 eV) was much larger than that of OH^- (530.2 eV) or H_2O (532.1 eV),[30] confirming that the film is mainly composed of oxide. In the N1s region, we detected a peak at 401.6 eV attributable to positively charged nitrogen[31,32] belonging to the cationic portion of C16 surfactant. Besides, the incorporation of Cl^- anions into the interlayer was recognized by doublet peaks assignable to the Cl $2p_{1/2}$ (197.8 eV) and Cl $2p_{3/2}$ (196.3 eV) states, along with the Cl 2s peak at 265 eV.[32,33] This finding enables us to realize that cationic heads of the incorporated surfactants are not only in coupling with negative charges on the MnO_2 layers but also in coupling with Cl^- anions. The atomic ratios of Cl/Mn and N/Mn were calculated to be 0.42 and 0.74, respectively, using the corrected areas of N 1s, Cl $2p_{3/2}$, and Mn $2p_{1/2}$ peaks. The fraction of the surfactants that interact with negative charges on MnO_2 layers can be estimated to be 0.32 by subtracting the Cl/Mn (0.42) ratio from the N/Mn (0.74) ratio. The obtained value, which corresponds to x in eq 1, is a typical value of chemically prepared K-birnessite.[9−11]

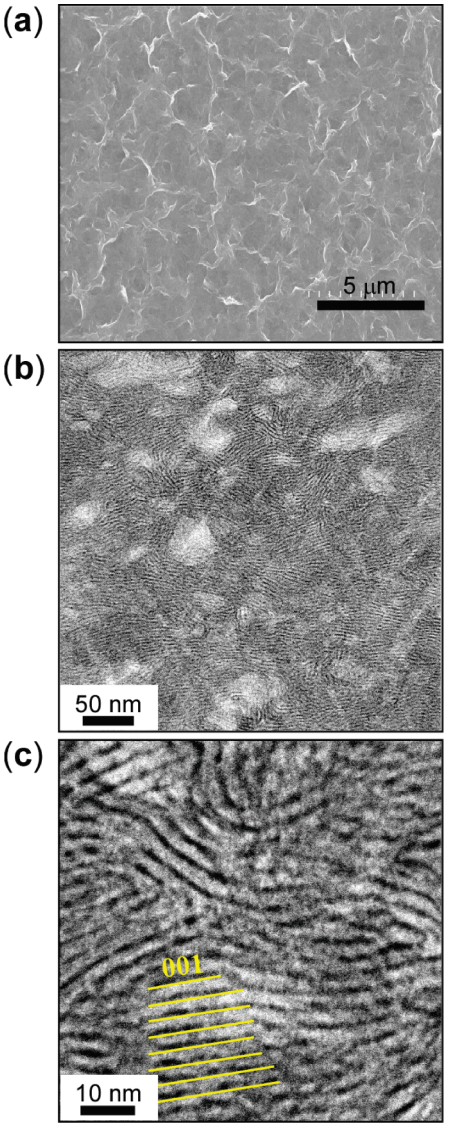

Figure 4. (a) Top-surface SEM and (b, c) cross-sectional TEM images of electrodeposited C16/MnO_2 film. The film was prepared by the same method as that of film a in Figure 2A.

Figure 4 shows top-surface SEM (a) and cross-sectional TEM (b and c) images of the C16/MnO_2 film. The relatively smooth surface appearing in Figure 4a is characteristic of the electrodeposited layered MnO_2 films.[19] Stripes at equal intervals are observed over the entire area, evidencing the electrochemical multilayer assembly. The dark stripes in Figure 4c correspond to MnO_2 layers, while the white stripes correspond to the layers composed of the assembled surfactants. The 001 planes are indicated in the picture, where the interlayer spacing is roughly estimated to be 3 nm, being close to the value obtained from the XRD data.

On the basis of XRD data for the films prepared at various surfactant concentrations (Supporting Information, Figure S2), the best products with respect to crystallinity were formed at 150 mM and 50 mM of C16 and C12,

(27) Allen, G. C.; Curtis, M. T.; Hopper, A. J.; Tucker, P. M. *J. Chem. Soc., Dalton Trans.* **1974**, *14*, 1525.
(28) Post, J. E.; Veblem, D. R. *Am. Mineral.* **1990**, *75*, 477.
(29) Wallin, T.; Linse, P. *J. Phys. Chem. B* **1997**, *28*, 5506.
(30) Casella, I. G.; Gatta, M. *Anal. Chem.* **2000**, *72*, 2969.
(31) Zahr, A. S.; Villiers, M.; Pishko, M. V. *Langmuir* **2005**, *21*, 403.
(32) Nakayama, M.; Tagashira, H. *Langmuir* **2006**, *22*, 3864.
(33) Usha, N.; Viswanathan, B.; Murthy, V. R. K.; Sobhanadri, J. *Spectrochim. Acta, Part A* **1997**, *53*, 1761.

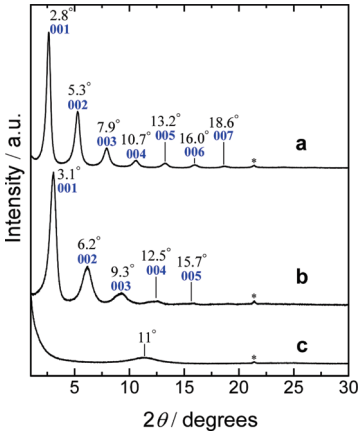

Figure 5. XRD patterns of the electrodeposited films (a) before and (b, c) after immersion for 24 h in (b) 0.5 M Na_2SO_4 and (c) ethanol. The film was prepared by the same method as that of film a in Figure 2A.

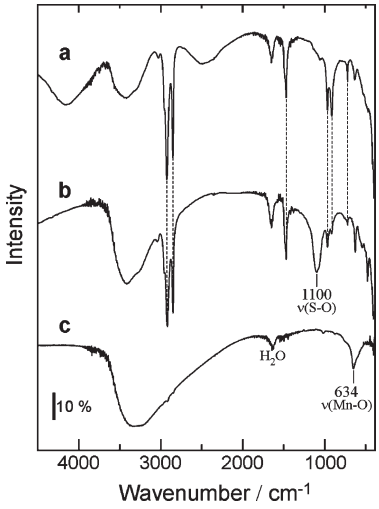

Figure 6. FTIR spectra of the electrodeposited films (a) before and (b, c) after immersion for 24 h in (b) 0.5 M Na_2SO_4 and (c) ethanol.

respectively. At these concentrations, both surfactants are present as micelles in bulk solutions,[34] which means that their assembly forms in bulk solution do not significantly affect the film formation process. This coincides with the finding reported by Huo et al., where surfactants pack parallel to provide high possible charge density to balance inorganic ions adsorbed on the electrode surface.[35]

Immersion in Aqueous Na_2SO_4 Solution and Ethanol. Figure 5 shows XRD patterns of the C16/MnO_2 film taken before (as-deposited) (a) and after being immersed in aqueous Na_2SO_4 solution (b) and ethanol (c). In the case of Na_2SO_4 solution, the diffraction pattern itself is basically the same as that of the as-deposited film, demonstrating that the C16 cations intercalated during electrodeposition are not replaced by small Na^+ ions but remain immobilized in the interlayer, probably due to the lateral interaction between the hydrophobic tails of surfactants. This observation is quite different from the birnessite film with tetrabutylammonium (Bu_4N^+) ions, where the intercalated Bu_4N^+ cations were rapidly replaced by smaller cations in solution, leading to a shrinkage of the interlayer spacing.[19] A slight shift of the diffraction peaks to the higher angles can be associated with the ion-exchange between Cl^- anions incorporated during electrodeposition and SO_4^{2-} in solution, as described later. The interlayer spacing of the film after immersion in Na_2SO_4 solution was estimated to be 2.8 nm. On the other hand, the immersion into ethanol caused a complete disappearance of the series of peaks, leaving a small bump centered at 11° in 2θ which corresponds to a repeating periodicity about 0.8 nm. Although this feature could not be assigned to any known structure, the crystalline structure of the film was largely lost.

The same samples were subjected to reflection absorption FTIR analysis, and the obtained spectra are displayed in Figure 6. As expected from the XRD data, the absorption peaks related to C16 remain unchanged after immersion in Na_2SO_4 solution (curve b), as indicated by dotted lines. The only difference is the occurrence of a peak at 1100 cm^{-1} attributable to the ν(S−O) vibrations in SO_4^{2-}.[36] This clearly indicates the replacement of Cl^- ions by SO_4^{2-}, probably as a result of strong and specific affinity of SO_4^{2-} to the C16 surfactant.[37] In the case of ethanol (curve c), conversely, the C16 absorptions completely disappear, leaving the broadened peak at 634 cm^{-1} due to the Mn−O stretching vibrations and the feature related to H_2O. Clearly, the anodically incorporated C16 surfactants can be extracted into the organic phase.

Electrochemical Properties. Figure 7A shows voltammograms of the C16/MnO_2 film when cycled repeatedly in an aqueous 0.5 M Na_2SO_4 electrolyte at a scan rate of 20 mV/s over the potential range 0 to +1.0 V. After 30 cycles, the film reached a steady-state where the oxidation/reduction of Mn^{3+}/Mn^{4+} ions in the oxide can take place reversibly.[38,39] The steady-state voltammogram exhibits a roughly rectangular image with no distinct redox peaks, which corresponds to a typical pseudocapacitive behavior where the current flow is independent of the electrode potential.[40,41] The specific capacitance (C, in farads per gram) was measured to be 193 F/g at a potential scan rate of 20 mV/s, according to

$$C = Q/(m\Delta E) \qquad (2)$$

where Q is the voltammetric charge (in coulombs) calculated by integrating the CV curve, m is the mass of the electroactive material (in grams), and ΔE is the potential window (in volts), respectively. The mass of the

(34) Acharya, D. P.; Hattori, K.; Sakai, T.; Kunieda, H. *Langmuir* **2003**, *19*, 9173.
(35) Huo, Q. S.; Margolese, D. I.; Cielsa, U.; Demuth, D. G.; Feng, P. Y.; Gier, T. E.; Sieger, P.; Firouzi, A.; Chmelka, B. F.; Schüth, F.; Stucky, G. D. *Chem. Mater.* **1994**, *6*, 1176.
(36) Mahadevan Pillai, V. P.; Nayar, V. U.; Jordanovska, V. B. *J. Solid State Chem.* **1997**, *133*, 407.
(37) Feitosa, E.; Brazolin, M. R. S.; Naal, R. M. Z. G.; Lama, M. P. F. M. D.; Lopes, J. R.; Loh, W.; Vasilescu *J. Colloid Interface Sci.* **2006**, *299*, 883.
(38) Toupin, M.; Brousse, T.; Bélanger, D. *Chem. Mater.* **2002**, *14*, 3946.
(39) Toupin, M.; Brousse, T.; Bélanger, D. *Chem. Mater.* **2004**, *16*, 3184.
(40) Lee, H. Y.; Goodenough, J. B. *J. Solid State Chem.* **1999**, *144*, 220.
(41) Nakayama, M.; Tanaka, A.; Sato, Y.; Tonosaki, T.; Ogura, K. *Langmuir* **2005**, *21*, 5907.

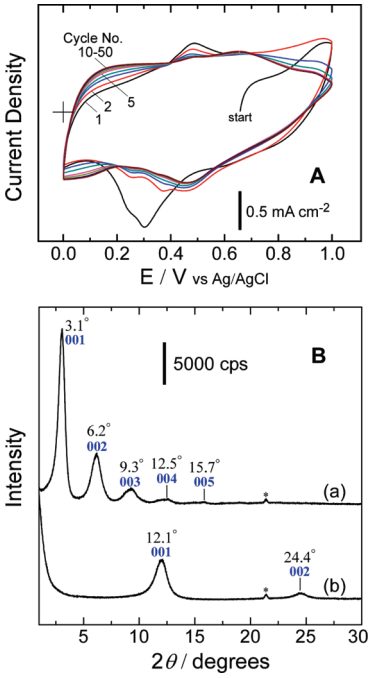

Figure 7. (A) Voltammograms of the C16/MnO_2 film electrode in a 0.5 M Na_2SO_4 solution as a potential scan rate of 20 mV/s. (B) XRD patterns of the C16/MnO_2 film taken after being immersed in a 0.5 M Na_2SO_4 solution (a) and then cycled in the same solution (b).

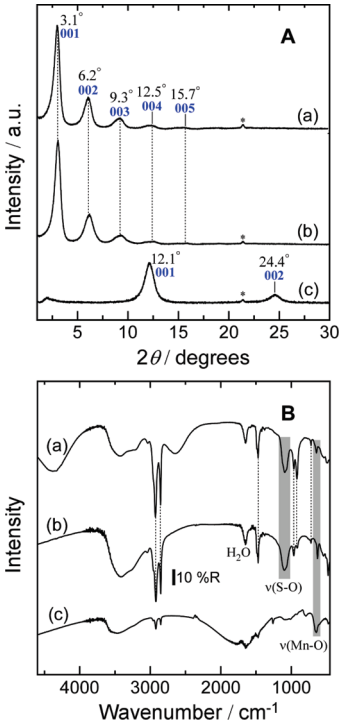

Figure 8. (A) XRD patterns and (B) FTIR spectra of the C16/MnO_2 film taken after being held for 30 min at (a) +1.0, (b) OCP, and (c) 0 V in a 0.5 M Na_2SO_4 solution.

electroactive material (as MnO_2) was calculated on the basis of the charge passed during electrodeposition. The specific capacitance value is similar to, or better than, those reported for chemically synthesized birnessite with conductive carbon.[21,22]

XRD pattern of the C16/MnO_2 film taken after 50 CV cycles is shown in Figure 7B(b), along with that before cycling (= after being immersed in Na_2SO_4 solution). After the potential cycling, new two peaks appear at 12.1° and 24.4° in 2θ, corresponding to d-spacings of 0.73 (d_{001}) and 0.36 (d_{002}) nm, respectively, while the characteristic peaks of the C16/MnO_2 structure disappear completely. Clearly, all the intercalated C16 cations are replaced with smaller Na^+ ions (0.19 nm)[42] in the electrolyte solution. In this case, the interlayer spacing (d_{001}) is determined by the size of water molecule (0.28 nm), which results in the shrinkage of the interlayer from 2.8 to 0.73 nm. Since the surfactants cannot be replaced with Na^+ ions in solution through a simple ion-exchanged mechanism, as mentioned above, they must be expelled electrochemically to balance the charge on the Mn oxide film during the redox reactions. The fact that all surfactants were replaced by Na^+ ions strongly suggests that the MnO_2 layers are electrochemically active and their internal surfaces are available for the intercalation of charge-compensating ions (Na^+) during redox processes.

To further elucidate the electrochemical properties, we investigated the film structure and surfactant behavior as a function of the applied potential. Figure 8 displays XRD patterns (A) and FTIR spectra (B) of the C16/MnO_2 films obtained after being held at open circuit potential (OCP, b) and anodic (a) and cathodic (c) potentials for 30 min in 0.5 M Na_2SO_4 electrolyte. Unexpectedly, the diffraction pattern of the film polarized at +1.0 V is the same as that taken at OCP. This can also be confirmed from the infrared absorptions arising from C16 and SO_4^{2-} (curves a and b in Figure 8B). On the other hand, the XRD pattern at 0 V is essentially the same as that obtained after CV cycling (Figure 7), suggesting the replacement of the interlayer by Na^+ ions. The corresponding FTIR spectrum also reveals the loss of both C16 and SO_4^{2-}.

All the above results can be explained schematically by Figure 9. The Cl^- anions incorporated during electrodeposition are ion-exchanged with SO_4^{2-} when the C16/MnO_2 film is immersed in Na_2SO_4 solution. Upon oxidation, Mn^{3+} ions in the oxide are converted to Mn^{4+}, leading to a decrease in negative charge of the MnO_2 layers, which can be compensated by the insertion of SO_4^{2-} anions, and not by the deintercalation of individual C16 cations. This phenomenon can be recognized by a unique property of surfactant molecules; i.e., they act collectively due to their hydrophobic interaction and do not act as individual ions above the critical aggregation (micelle) concentration (1.35 mM in the absence of additional salt[43]). In this situation, the newly inserted SO_4^{2-} anions are coupled with the cationic heads of the surfactants that became unnecessary to balance the negative charges on the MnO_2 layers. Upon reduction, there are two possibilities to balance the increased negative charge on the MnO_2 layers due to the conversion of some Mn^{4+} ions to Mn^{3+} ions: (i) the SO_4^{2-} ions intercalated in the

(42) Shannon, R. D. *Acta Crystallogr., Sect. A: Cryst. Phys., Diffr., Theor. Gen. Crystallogr.* **1976**, *A32*, 751.

(43) Sepulveda, L.; Cortes, J. *J. Phys. Chem.* **1985**, *89*, 5322.

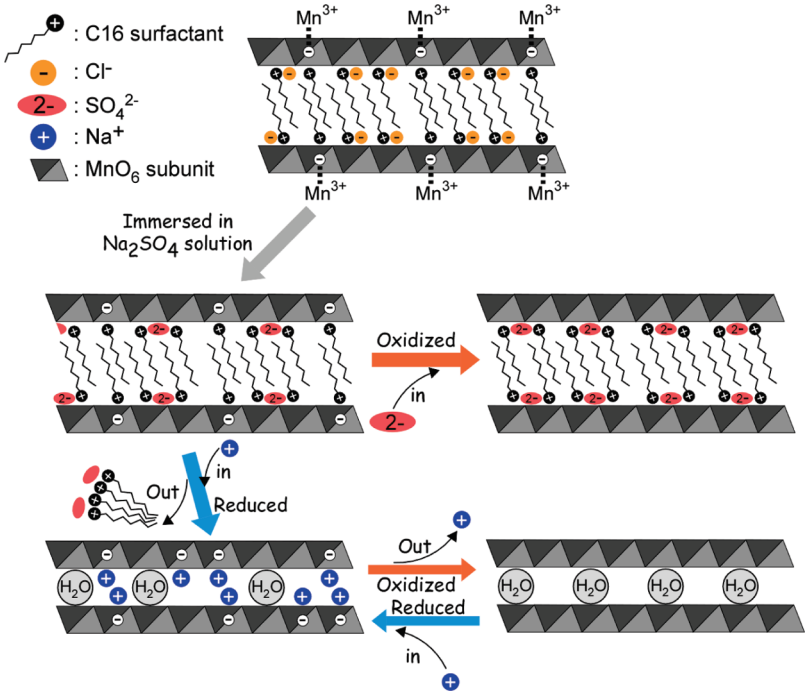

Figure 9. Schematic illustration of the electrochemical behavior that takes place in the C16/MnO_2 film.

interlayer go out to leave C16 cations or (ii) Na^+ ions in solution are inserted. The latter process coincides with the obtained results, probably because of the specific and strong affinity of SO_4^{2-} to C16, as described above. The insertion of Na^+ ions can cause simultaneous deintercalation of all the surfactants together with SO_4^{2-}. Once Na^+ ions are inserted, they can play a role of the charge-compensating ions in the redox mechanism of MnO_2,[39] which is responsible for the steady state voltammetric response after 30 cycles in Figure 7A. The fact that C16 cations remain immobilized between the MnO_2 layers at anodic potentials prompted us to examine the use of the resulting film electrode for the oxidation of hydroquinone (HQ) within the large interlayer space.

Oxidation of Phenol. *In situ* absorption spectra of HQ were acquired in 0.5 M Na_2SO_4 electrolyte, while the C16/MnO_2 film-coated ITO electrode was polarized at a constant potential of +1.0 V. Time courses of the UV−vis absorption spectra are shown in Figure 10, taken with (a) and without (b) polarization. HQ provides an absorption peak at 288 nm which is attributable to $\pi-\pi^*$ transition.[44] Regardless of the polarization state, the absorption at 255 nm due to *p*-benzoquinone (*p*-BQ) increases with time, indicating two-electron oxidation of HQ with the high-valent Mn sites (Mn^{4+}) to *p*-BQ. In the inset, the residual HQ and the conversion of HQ to BQ are plotted as a function of reaction time, where each plot represents the average of three experiments. The initial rate of HQ oxidation is apparently enhanced by polarizing the film electrode.

Figure 11 depicts *i-t* plots of the C16/MnO_2/ITO electrode when polarized at +1.0 V in 0.5 M Na_2SO_4 solution with (a) and without (b) HQ. As a control experiment, the

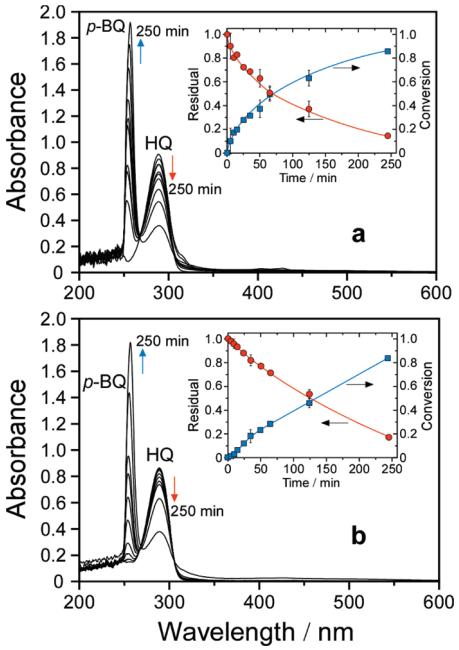

Figure 10. Time courses of UV−vis absorption spectra of HQ at 0.3 mM in 0.5 M Na_2SO_4 solution while the C16/MnO_2 film was kept at (a) +1.0 V and (b) OCP.

oxidation of HQ was similarly conducted using a bare ITO electrode (curve c). The film-modified electrode exhibits an enhancement of oxidation current 684 times larger than the unmodified ITO electrode. The current in the absence of HQ is hardly observed, thus indicating that HQ is oxidized catalytically at the C16/MnO_2 film electrode.

XRD patterns shown in Figure 12 were taken after the HQ oxidation at +1.0 V (a) and OCP (b). Surprisingly, although the reaction at OCP results in a collapse of the C16-intercalated structure, the anodic polarization allows

(44) Carter, M. K. *J. Mol. Struct.* **2007**, *831*, 26.

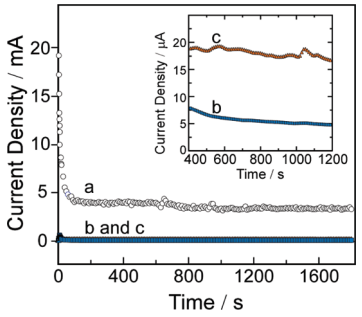

Figure 11. *i-t* plots obtained when (a, b) C16/MnO_2 film-modified and (c) unmodified ITO electrodes were polarized at +1.0 V in 0.5 M Na_2SO_4 solution (a, c) with and (b) without 0.3 mM HQ.

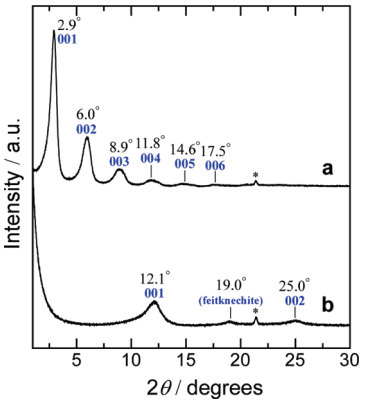

Figure 12. XRD patterns of the C16/MnO_2 films on an ITO electrode after being polarized for 250 min at (a) +1.0 V and (b) OCP in a Na_2SO_4 solution containing 0.3 mM HQ.

the structure to remain unchanged. Since the surfactants cannot be ion-exchanged with Na^+ ions, the removal of C16 cations at OCP strongly suggests that the HQ oxidation takes place within the interlayer space. The HQ oxidation proceeds accompanied with the reduction of Mn^{4+} to Mn^{3+}, which leads to an increase in negative charge to be compensated by electrolyte Na^+ ions. The surfactants are expelled as soon as they become unnecessary, as in the case when the C16/MnO_2 film is reduced (curves c in Figure 8). A peak at 19.0° can be attributed to β-$Mn^{III}OOH$ (feitknechite),[45] indicating the presence of the reduced Mn species. When the electrode is polarized positively, however, the generated Mn^{3+} sites are oxidized back to Mn^{4+}, keeping the net negative charge in the Mn oxide film so that the surfactants are not necessary to be deintercalated. That is, electrons are transferred from HQ to the substrate electrode through the MnO_2 layers, which provides catalytic current. In other words, the MnO_2 layers can act as mediators for the HQ oxidation taking place in the large interlayer space composed of the assembled C16 surfactants.

(45) Luo, J.; Zhang, Q.; Suib, S. L. *Inorg. Chem.* **2000**, *39*, 741.

Conclusions

Multilayered manganese oxides intercalated with surfactant molecules were electrodeposited from an aqueous $MnSO_4$ solution containing cationic surfactants. The C16 to MnO_2 molar ratio was estimated to be 0.74, in which the fraction interacting with negative charges on the MnO_2 layers is 0.32. The intercalated C16 surfactants were not ion-exchanged with Na^+ ions in solution but extracted with ethanol. When the C16/MnO_2 film was oxidized in Na_2SO_4 electrolyte, a decrease in net negative charge can be compensated by the insertion of SO_4^{2-} anions, and not by the deintercalation of the surfactant cations. The C16/MnO_2 film effectively oxidized HQ to *p*-BQ within the interlayer space, while the Mn^{4+} sites in the oxide were reduced to Mn^{3+}. Although the accumulation of the low-valent Mn species resulted in the collapse of the C16-intercalated layered structure, applying an anodic potential to the film electrode allowed the crystalline structure to remain unchanged, in conjunction with acceleration of the HQ oxidation. The current observed for the catalytic oxidation of HQ on the C16/MnO_2 film electrode was 684 times larger than that observed on the unmodified electrode.

Acknowledgment. This research was supported in part by the Japan Society of the Promotion of Science (No. 20550180). We thank Prof. Hidetoshi Kita with XPS measurements.

Supporting Information Available: XPS of the film deposited from $MnSO_4$ solution containing C16 (Figure S1) and XRD patterns of the MnO_2 films deposited with C16 and C12 surfactants at various concentrations (Figure S2). This material is available free of charge via the Internet at http://pubs.acs.org.